

Influence of Zeolites on the Sintering and Technological Properties of Porcelain Stoneware Tiles

Roberto de' Gennaro^a, Piergiulio Cappelletti^a, Guido Cerri^a, Maurizio de' Gennaro^a, Michele Dondi^b, Guia Guarini^b, Alessio Langella^c, Debora Naimo^a

^a*Dipartimento di Scienze della Terra, Università Federico II, via Mezzocannone 8, 80138 Naples (Italy)*

^b*Istituto di Scienza e Tecnologia dei Materiali Ceramici (CNR-ISTEC), via Granarolo 64, 48018 Faenza (Italy)*

^c*Dip.to di Studi Geologici ed Ambientali, Università del Sannio, Via Port'Arsa 11, 82100 Benevento (Italy)*

Abstract

Low-cost zeolitic rocks are promising substitutes for feldspathic fluxes in ceramic bodies, since their fusibility, [searce-modest](#) hardness and high cation exchange capacity (CEC) should improve grinding and sintering. Five large-scale Italian deposits of natural zeolites with different mineralogy were characterised and tested in porcelain stoneware bodies. Their behaviour during processing was appraised and compared with that of zeolite-free bodies. Zeolites increased the slip viscosity during wet grinding, causing a coarser grain size distribution and consequently some drawbacks in both unfired and fired tiles. After overcoming this hindrance by dry grinding of zeolite rocks, the technological behaviour of zeolite-bearing tiles appear to be similar to that of current porcelain stoneware, though with larger firing shrinkage and residual closed porosity.

Keywords: Sintering; Traditional ceramics; Zeolites; Porcelain stoneware; Tiles.

1. Introduction

Over the last decade, the Italian ceramic tile industry has progressively shifted its production toward new materials with excellent technical properties, i.e. porcelain stoneware tiles.¹⁻² These products are manufactured using large amounts of fluxes, such as sodic and potassic feldspars,³ nepheline syenite,⁴ talc,⁵⁻⁶ borates,⁷ wollastonite,⁸ and recently even glass-ceramic frits.⁹⁻¹⁰

The high price of these raw materials has a remarkable impact on the cost of the end-product, making Italian tile manufacture disadvantaged in competition with that of other tilemaking countries where production costs are lower. This fact drove the Italian industry to a continuous search for cheap raw materials able to replace the traditional fluxes without altering the process and product characteristics.¹¹

Zeolite-rich rocks could effectively represent suitable low-cost materials, since large deposits of natural zeolites occur in Italy.¹² Moreover, some technological features of zeolites (e.g. low melting temperatures, low hardness and high cation exchange capacity) should ensure a considerable improvement in the grinding and firing stages of the tilemaking cycle, though contrasting results emerged from previous investigations.¹³⁻¹⁴

This study is aimed at assessing the influence of zeolites on both the technological behaviour during processing and the technical performances of porcelain stoneware tiles. A wide spectrum of naturally-occurring zeolitized materials was taken into account, in order to evaluate the effect of different zeolites (chabazite, analcite, phillipsite, clinoptilolite) and chemico-physical properties (specific surface, cation exchange capacity).

The experimental approach consisted in a laboratory simulation of the tilemaking process carried out by replacing conventional fluxes (sodic feldspar and potassic aplite) with zeolitic rocks in typical porcelain stoneware bodies. The characteristics of both semi-finished and finished products were appraised comparing zeolite-bearing formulations with a reference zeolite-free body.

2. Materials

Five large-scale deposits of zeolite-rich rocks (ignimbrites, tuffs, epiclastites) were taken into consideration, sampling covering of the following geological units in Central and Southern Italy: the Sorano Formation (IS), the Neapolitan yellow tuff (TGN), the Campanian ignimbrite (IC), the Bortivuille (LB) and Sa Contra (ESC) sediments.

The *Sorano Formation*¹⁵⁻¹⁷ is extensively zeolitized, with chabazite prevailing on minor phillipsite; zeolite content ranges from about 60% to 70%.¹⁸ The sample IS was collected at the Pian di Rena quarry (Sorano, Grosseto, Tuscany).

The Neapolitan yellow tuff is the product of a huge eruption that took place about 12,000 years ago within the volcanic area of Campi Flegrei. The total zeolite content is almost always higher than 50%, with the phillipsite content much higher than chabazite and analcime.¹⁹ The sample TGN was collected in Grotta del Sole locality (Quarto, Naples, Campania).

The Campanian Ignimbrite is the product of another eruption of Campi Flegrei (37,000 years ago) which gave rise to two different lithofacies,²⁰ the yellow one being characterized by the presence of chabazite, though some deposits or particular layers can be found with a similar content of phillipsite. The zeolite amount is generally close to 50%, although in some deposits it can even reach about 80%.²¹ The sample IC was collected in S. Nicola la Strada (Caserta, Campania).

Both Bortivuille and Sa Contra epiclastites, outcropping in Northern-Central Sardinia, belong to a fluvio-lacustrine sedimentary deposit affected by secondary mineralization processes which led to the formation of zeolite, opal-CT and smectite.²²⁻²⁴ The zeolite occurring in these rocks is, in most cases, a clinoptilolite, whose amount ranges between about 30% and 80%.²³ Samples LB and ESC were collected at Bortivuille (Sassari) and Sa Contra (Sassari), respectively.²⁵

In the laboratory trials, typical porcelain stoneware bodies²⁶ were reproduced with raw materials currently used by the Italian tilemaking industry (Table 1). In particular, ball clays from Westerwald, Germany (W1, W2 and W3), Donbass, Ukraine (U1 and U2), and Sardinia, Italy (F1) were admixed with quartz-feldspathic fluxes, such as sodic feldspar from Sardinia, Italy (SF1) and Southwestern Anatolia, Turkey (SF2), potassic aplite from Tuscany, Italy (AP) and arkosic sand from Northern Apennines, Italy (QFS).

3. Methods

The mineralogy of the zeolitic rocks was investigated by X-ray powder diffraction (XRPD, Philips, PW 1730/3710, Cu K α radiation) performing the quantitative interpretation of XRD patterns by both the Reference Intensity Ratio²⁷ and the Rietveld techniques.²⁸ Chemical analyses of raw materials and ceramic bodies were performed by inductively-coupled plasma optical emission spectrometry (ICP-OES, Varian, Liberty 200) after alkaline fusion with lithium tetraborate in graphite crucible.²⁹

The following properties of the zeolitic materials were determined: cation exchange capacity by ICP-OES after exchange with ammonium chloride;³⁰ specific surface by

nitrogen adsorption (ASTM C 1069); fusibility and firing behaviour by hot-stage microscopy with a thermal rate of $10^{\circ}\text{C min}^{-1}$.³¹

The technological behaviour of ceramic bodies was assessed by simulating, at a laboratory scale, the tilemaking process and by characterizing both the semi-finished and finished products. The porcelain stoneware bodies were designed by replacing two conventional feldspathic fluxes (10% each of potassic aplite and sodium feldspar) with 20% zeolitic rock (Table 2). Two routes of body preparation were followed:

- the raw materials of bodies Nz, Z1, Z2, Z3, Z4 and Z7 were mixed and wet ground all together in a porcelain jar with dense alumina grinding media (18 hours);
- the ball clays and quartz-feldspathic fluxes of bodies Z0, Z5 and Z6 were wet ground as above, while the zeolitic rock was dry ground separately (under 0.25 mm in hammer mill) and successively added to the slip.

The slips were dried in an oven ($105\pm 5^{\circ}\text{C}$), then the powders were deagglomerated by hammer milling and pelletized after adding water (5-7% wt). After adequate storage, $110 \cdot 55 \cdot 5 \text{ mm}^3$ tiles were prepared by pressing (40 MPa), drying in an oven ($105\pm 5^{\circ}\text{C}$) and fast firing in an electric roller kiln at four maximum temperatures in the $1100\text{-}1180^{\circ}\text{C}$ range for 60 minutes cold-to-cold.

The particle size distribution of the slips was analysed by photosedimentation (ASTM C 958). Working moisture (ASTM C 324) and compressibility (mould depth/tile thickness ratio) were determined on the powders. Green and dry tiles were characterized by measuring pressing expansion, drying shrinkage (ASTM C 326) and modulus of rupture (ISO 10545-4).

Firing shrinkage (ASTM C 326), water absorption, open porosity and bulk density (ASTM C 326), and 3-points modulus of rupture (ISO 10545-4) were measured on fired tiles. Closed porosity was determined by the ratio between bulk density and specific weight of the ceramic material (ASTM C 329).

The quantitative phase composition of fired tiles was determined by XRPD (Rigaku, Miniflex, $\text{CuK}\alpha$ radiation) with the RIR method using CaF_2 as internal standard. The chemical composition of the glassy phase was calculated on the basis of the bulk chemistry and phase composition of tiles. The viscosity and surface tension of the glassy phase were estimated on the basis of chemical composition.³²⁻³³

4. Results and discussion

4.1. Properties of zeolitic raw materials

The zeolitic rocks taken into account present different chemical features, particularly samples IS, TGN and IC on one side and samples LB and ESC on the other side. The former are characterized by a low $\text{SiO}_2/\text{Al}_2\text{O}_3$ ratio and remarkable amounts of K_2O , CaO and Fe_2O_3 ; the latter are richer in silica and poorer in aluminium, iron, alkaline and alkaline-earth oxides (Fig. 1 and Table 3). At all events, iron content is considerably higher than in conventional feldspathic fluxes ($\text{Fe}_2\text{O}_3 < 1\%$).

Zeolites are the major components, ranging between 55% and 66%, excluding sample ESC. Different zeolites characterize every material: chabazite (IS), chabazite + phillipsite (IC), clinoptilolite (LB and ESC), phillipsite + chabazite + analcime (TGN). Furthermore, sample ESC is characterized by a high feldspar content. Opal, smectite and volcanic glass are sometimes present in noteworthy quantities (Table 3).

The values of specific surface ($38\text{-}225 \text{ m}^2 \cdot \text{g}^{-1}$) and cation exchange capacity (CEC $64\text{-}130 \text{ meq}/100\text{g}$) are very high compared with those of conventional ceramic raw materials³⁴ and they depend to a large extent on the amount and type of zeolites and associated phases, particularly smectite (Table 3).

These zeolitic rocks are more easily fusible than most quartz-feldspathic fluxes: softening (T_3) begins between 1200 and 1280 °C, while melting (T_4) occurs in the 1320-1470 °C range (Table 4). The firing behaviour depends basically on the composition: chabazite-phillipsite materials, richer also in iron oxide, exhibit the lowest temperatures, somehow comparable with nepheline syenite, while clinoptilolite compositions are slightly less fusible, with characteristic temperatures similar to sodic feldspar.³¹ In particular, the phillipsite-rich sample TGN presents the lowest sintering and softening temperatures, but the 'melting point' is slightly higher than that of chabazite-rich zeolitites (IS and IC). As far as epiclastites are concerned, the lower clinoptilolite amount of sample ESC translates in an upward shift of 10-30 °C on all characteristic temperatures. Samples LB and TGN tend to bloat significantly before melting, approximately doubling their volume in the T_3 - T_4 range.

4.2. Behaviour of semi-finished products

The introduction of zeolites in porcelain stoneware bodies brought about a relevant variation in slip rheology, causing a considerable increase of viscosity and consequently a proportional decrease of grinding efficiency. Wet ground zeolite-bearing bodies (Z1, Z2, Z3 and Z4) have a clearly different particle size distribution in respect of the reference body (NZ) with the exception of sample Z7. As a matter of fact: the higher the values of specific surface of the zeolitite added, the coarser the particle size of the ceramic body (Fig. 2).

The grinding performance was affected also by the zeolite type, as can be appreciated by ordering the wet ground samples in decreasing mean particle size: IS (chabazite), IC (chabazite > phillipsite), TGN (phillipsite > chabazite), LB (clinoptilolite > feldspar), ESC (clinoptilolite ~ feldspar). This behaviour depends on the CEC and probably on a complex balance between the exchangeable alkaline and alkaline-earth elements, the latter having a well known effect on slip viscosity.³⁵⁻³⁶

In order to avoid any interference of the zeolites on wet grinding, a second series of porcelain stoneware bodies was prepared by milling separately the zeolitic raw material and the rest of the body (Z0, Z5 and Z6), getting a suitable particle size distribution, though still slightly rich in the coarser fraction (approximately 7% >63 µm).

No particular problem occurred during the pressing and drying stages: the presence of zeolites did not change significantly either the pressing expansion or the drying shrinkage, while the modulus of rupture is generally increased, especially in the case of green tiles, notwithstanding the different particle size distribution (Table 5).

4.3. Firing behaviour

The relatively coarse granulometry of the wet ground zeolite-bearing bodies (Z1, Z2, Z3 and Z4) deeply affected their firing behaviour, producing clearly lower values of linear shrinkage and mechanical strength as well as larger values of porosity with respect to the reference body NZ. The ranking of bodies corresponds well to their particle size distribution, with those containing the chabazite-rich zeolitites more distant from the reference (Fig. 3).

A more significant comparison is made possible by considering the samples with particle size distributions analogous to those of industrial porcelain stoneware bodies (i.e. Z0, Z5, Z6 and Z7). In this case, bodies Z5 and Z6 contain more zeolites (11% and 13% respectively) than body Z7 (approximately 7%) and they exhibit a different behaviour (Tables 6 and 7):

- clearly higher firing shrinkage, for the same porosity;
- lower bulk density, for the same water absorption;
- significant amounts of closed porosity;
- lower modulus of rupture.

The persistence of closed porosity in sintered tiles can to a large extent explain the lower values of bulk density and mechanical strength in respect of the reference body.³⁷⁻³⁸ The larger shrinkage of the zeolite-bearing bodies is probably explained by an increase of both the liquid phase during the viscous flow sintering and the porosity formed during firing due to the larger loss on ignition (Table 7).

On the other hand, the body Z7 is characterized by values of bulk density, modulus of rupture, open and closed porosity absolutely comparable with those of industrially manufactured tiles.³⁸ In this case too, firing shrinkage is higher than that of current porcelain stoneware bodies (Table 6).

4.4. Phase composition

The replacement of zeolites for feldspathic fluxes produced a noticeable change in the phase composition of porcelain stoneware tiles (Fig. 4). In particular, the occurrence of zeolites brought about:

- smaller amounts of residual quartz and feldspar,
- slower dissolution rates of quartz and plagioclase in the 1120-1180 °C range,
- larger amount of mullite, though the differences are generally within the error of measurements,
- larger quantity of glassy phase.

The chemical composition of this glassy phase changed continuously with the increasing firing temperature (Table 8). In fact, as quartz and feldspar progressively melted, the liquid phase enriched in silica and soda, so diluting its concentration in Al_2O_3 (due also to mullite formation) as well as K_2O , MgO , CaO and Fe_2O_3 , that appeared to be dissolved in the melt already at 1120 °C. The overall trend consists in an increase with firing temperature of both silica/alumina and alkali/alumina ratios (Fig. 5). However, while the $(\text{Na}_2\text{O}+\text{K}_2\text{O})/\text{Al}_2\text{O}_3$ ratio is quite similar in all bodies, the $\text{SiO}_2/\text{Al}_2\text{O}_3$ ratio is remarkably higher in bodies Z6 and Z7, which contain relatively silica-rich clinoptilolite epiclastites. Moreover, both the reference and the Z7 bodies present a higher Na/K ratio.

All these chemical fluctuations affected the most important physical factors controlling the sintering rate, i.e. viscosity and surface tension of the liquid phase (Table 8). As a matter of fact, increasing the firing temperature:

- viscosity decreased with a faster rate in the zeolite-free body in respect to zeolite-bearing ones, due to the different alkali content and $\text{SiO}_2/\text{Al}_2\text{O}_3$ ratio;
- surface tension had negligible variations in all samples.

5. Conclusion

Zeolitized volcanoclastic and epiclastic deposits represent an important raw material for diverse application in different technological sectors, a major advantage being the low costs. Many deposits are exploited as sources of building materials either as cut stones or as additives in pozzolanic cements or special plasters. This large utilization brings about the production of a large amount of by-products, mainly deriving by quarrying operations.

This quarry dust could find a profitable application as a ceramic raw material, substituting for traditional fluxes, because of its fusibility, modest hardness and low cost. However, limits for this application concern:

- the high specific surface and CEC (that cause a worsening of the rheological behaviour of slips),
- the high Fe_2O_3 content (promoting a darkening of colour),
- the high loss on ignition (that brings about a larger firing shrinkage),

- the different chemico-physical features of the liquid phase at sintering temperature, which can explain the larger amounts of residual closed porosity.

Rocks containing zeolites and feldspars in similar amounts (such as ESC epiclastite) represent a promising compromise, that do not suffer many of the drawbacks of zeolite-rich materials.

References

1. Manfredini, T., Pellacani, G. C. and Romagnoli, M., Porcelainized stoneware tiles. *Am. Ceram. Soc. Bull.*, 1995, **74** (5) 76-9.
2. Burzacchini, P., Porcelain tile, its history and development. *Ceram. World Rev.*, 2000, **10** (37) 96-103.
3. Dondi, M., Compositional parameters to evaluate feldspathic fluxes for ceramic tiles. *Tile & Brick Int.*, 1994, **10** (2) 77-84.
4. Balkwill, S. and Bougher, A. K., Arkansas nepheline syenite as an alternative economic fluxing agent in ceramic formulations. *Ceram. Eng. Sci. Proc.*, 2001, **22** (2) 77.
5. Grosjean, P., CV3 Piedra and SSB 60: two white and extra white talcs to reduce the firing cost of porcelain stoneware tiles. *Int. Ceram. J.*, 2001, April, 63-66.
6. Dondi, M., Biasini, V., Guarini, G., Raimondo, M., Argnani, A. and Di Primio, S., The influence of magnesium silicates on technological behaviour of porcelain stoneware tiles. *Key Engineering Materials*, 2002, **206-213**, 1795-98.
7. Moreno, A., Garcia-Ten, J., Bou, E., Gozalbo, A., Simon, J., Cook, S. and Galindo, M., Using boron as an auxiliary flux in porcelain tile compositions. In *Proceedings of the 4th World Congress on Ceramic Tile Quality - QUALICER*, 2000, pp. P.GI 77-91.
8. Manfredini, T., Romagnoli, M. and Hanuskova, M., Wollastonite as sintering aid for porcelain tile bodies. *Int. Ceram. J.*, 2000, December, 61-7.
9. Moreno, A., Garcia-Ten, J., Sanz, V., Gozalbo, A., Cabedo, J., Berge, R., Colom, J. and Carmena, S., Feasibility of using frits as raw materials in porcelain tile compositions. In *Proceedings of the 4th World Congress on Ceramic Tile Quality - QUALICER*, 2000, pp. 237-51.
10. Baldi, G., Generali, E., Rovatti, L. and Settembre Blundo, D., Synthetic raw materials for bodies with a high whiteness index. *Ceram. World Rev.*, 2001, **11** (42) 72-80.
11. Sezzi, G., Raw materials for a global industry, *Ceram. World Rev.*, 1999, **9**, 106-9.
12. de' Gennaro, M. and Langella, A., Italian zeolitized rocks of technological interest. *Mineral. Deposita*, 1996, **31**, 452-472.
13. Andreola, F., Manfredini, T., Passaglia, E., Pellacani, G. C., Pozzi, P. and Romagnoli, M., Utilization of an italian zeolitite in ceramic bodies. *Materials Engineering*, 1994, **5**, 299-312.
14. Di Bartolomeo, P., Dondi, M. and Marsigli, M., Use of zeolitic rocks in ceramic tile production. *Tile & Brick Int.*, 1996, **12** (4) 311-18.
15. Sparks, R.S.J., Stratigraphy and geology of the ignimbrites of Vulsini Volcano, Italy. *Geol. Rund.*, 1975, **64**, 497-523.
16. Nappi, G., Stratigrafia e petrografia dei Vulsini sud-occidentali (caldera di Latera), *Boll. Soc. Geol. It.*, 1969, **88**, 171-181.
17. Vezzoli, L., Conticelli, S., Innocenti, F., Landi, P., Manetti, P., Palladino, D.M. and Trigila, R., Stratigraphy of the Latera Volcanic Complex: proposal for a new nomenclature. *Per. Mineral.*, 1987, **56**, 89-110.
18. Cappelletti, P., Langella, A., Colella, A. and de' Gennaro, R., Mineralogical and technical features of zeolite deposits from northern Latium volcanic district. *Per. Mineral.*, 1999, **68**, 127-144.
19. de' Gennaro, M., Cappelletti, P., Langella, A., Perrotta, A. and Scarpati, C., Genesis of zeolites in the Neapolitan Yellow Tuff: geological, volcanological and mineralogical evidence. *Contrib. Mineral. Petrol.*, 2000, **139**, 17-35.
20. Di Girolamo, P., Petrografia dei tufi campani: Il processo di pipernizzazione (Tufo → tufo pipernoide → piperno). *Rend. Acc. Sc. Fis. Mat. (Napoli)*, 1968, **35**, 329-393.
21. Buondonno A., Calcaterra D., Cappelletti P., Langella A., Nappi G., Perrotta A. and Scarpati C., International Committee on Natural Zeolites - "Zeo-trip '97 - An excursion to selected zeolite deposits in Central-Southern Italy"., Napoli, September 27-29, De Frede ed, 1997, pp. 69.
22. Cerri, G., Caratterizzazione mineralogica e tecnologica dei tufi zeolitizzati della Sardegna settentrionale. PhD thesis, University of Sassari, 2000.
23. Langella, A., Cappelletti, P., Cerri, G., Bish, D. L. and de' Gennaro, M., Distribution of industrial minerals in Sardinia (Italy): Clinoptilolite bearing rocks of Logudoro region. In *Natural Microporous Materials in*

Environmental Technology, Kluwer Academic Publishers, Dordrecht, The Netherlands, 1999, pp. 237-252

24. Cerri, G., Cappelletti, P., Langella, A. and de' Gennaro, M., Zeolitization of Oligo-Miocene volcanoclastic rocks from Logudoro (Northern Sardinia, Italy). *Contrib. Mineral. Petrol.*, 2001, **140**, 404-421
25. Cerri, G. and Oggiano, G., Le epiclastiti zeolitizzate del Logudoro orientale: un livello guida all'interno della successione vulcano-sedimentaria della Sardegna centrosettentrionale. *Boll. Soc. Geol. It.*, 2002, **121**, 3-10.
26. Dondi, M., Ercolani, G., Melandri, C., Mingazzini, C. and Marsigli, M., The chemical composition of porcelain stoneware tiles and its influence on microstructural and mechanical properties. *Interceram*, 1999, **48** (2) 75-83.
27. Bish, D. L. and Chipera, S. J., Problems and solutions in quantitative analysis of complex mixture by X-ray powder diffraction. *Adv. X-ray Anal.*, 1988, **31**, 295-307.
28. Bish, D. L. and Post, J. E., Quantitative mineralogical analysis using the Rietveld full-pattern fitting method. *Am. Mineral.*, 1993, **78**, 932-940.
29. Mingazzini, C., Dondi, M. and Fabbri, B., L'analisi chimica degli smalti e delle fritte ceramiche mediante spettrometria di emissione al plasma (ICP-AES). *Ceram. Inf.*, 1998, **379**, 343-8.
30. Federico Goldberg, L., Arduino, E., Metodi normalizzati di analisi del suolo. Edagricole, 1985, pp. 1-100.
31. Dondi, M., Guarini, G. and Venturi, I., Assessing the fusibility of feldspathic fluxes for ceramic tiles by hot stage microscope. *Industrial Ceramics*, 2001, **21**, 67-73.
32. Lakatos, T., Johansson, L. G. and Skimmingskold, B., Viscosity temperature relations in the glass systems. *Glass Technol.*, 1972, **6**, 88-95.
33. Cambier, F. and L  riche, A., Vitrification. In *Processing of Ceramics*, eds. R.W. Cahn, P. Haasen, E.J. Kramer. VCH, Weinheim, 1996, **17B**, Part II, pp. 123-44.
34. Dondi, M., Guarini, G. and Fabbri, B., Specific surface of clay raw materials used in the Italian ceramic industry. *Industrial Ceramics*, 1998, **18**, 149-53.
35. Carty, WM; Rossington, K., Correlating suspension rheology with suspension chemistry in a clay-based system. *Ceram. Eng. Sci. Proc.*, 2000, **21** (2), 127-38.
36. Paredes, C. A. and Haber, R. A., Effect of soluble ions on the rheological stability of clay slurries. *Ceram. Eng. Sci. Proc.*, 2001, **22** (2), 89-96.
37. Leonelli, C., Bondioli, F., Veronesi, P., Romagnoli, M., Manfredini, T., Pellacani, G. C. and Cannillo, V., Enhancing the mechanical properties of porcelain stoneware tiles: a microstructural approach. *J. Eur. Ceram. Soc.*, 2001, **21**, 785-93.
38. Biasini, V., Dondi, M., Guicciardi, S., Melandri, C., Raimondo, M., Generali, E. and Settembre Blundo, D., Mechanical properties of porcelain stoneware tiles: the effect of glass-ceramic systems. *Key Engineering Materials*, 2002, **206-213**, 1799-1802.

Fig. 1. Chemical composition of the zeolitic rocks: A) SiO_2 - Al_2O_3 - Alkaline-earth oxides ($\text{MgO}+\text{CaO}+\text{SrO}+\text{BaO}$); B) Fe_2O_3 - Alkaline oxides ($\text{Na}_2\text{O}+\text{K}_2\text{O}$) - Alkaline-earth oxides.

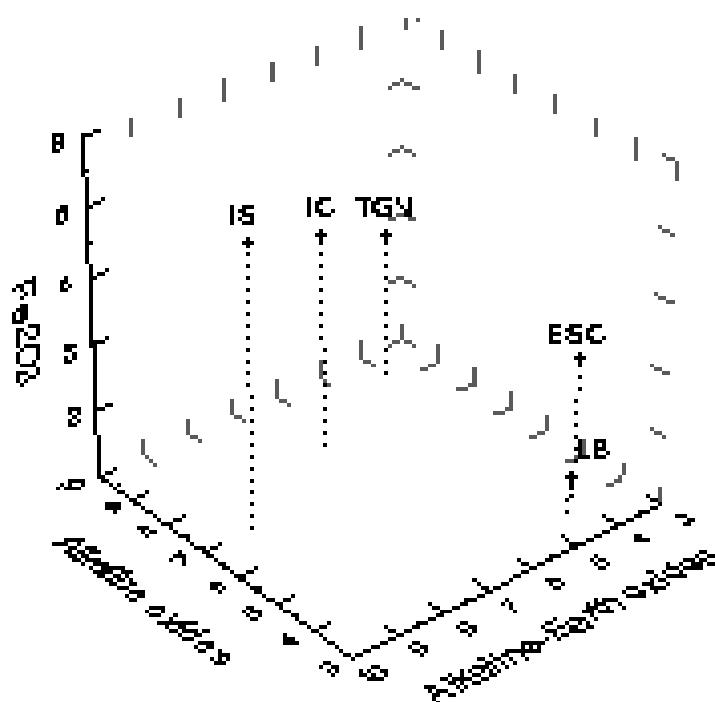
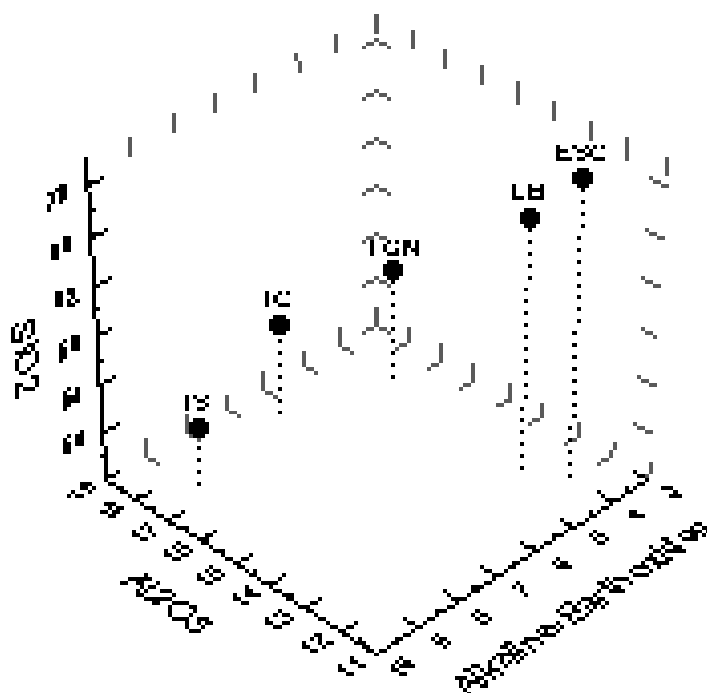


Fig. 2. Particle size distribution of bodies for porcelain stoneware tiles.

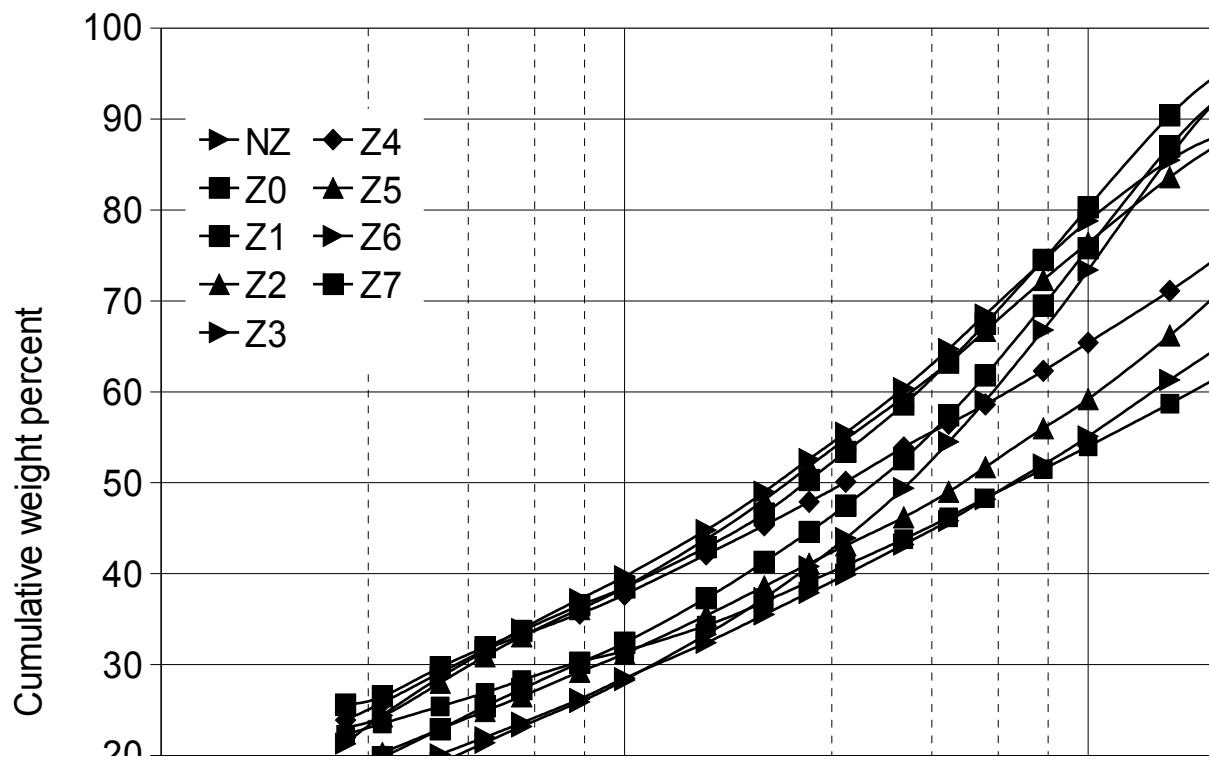


Fig. 3 Firing behaviour of wet ground bodies for porcelain stoneware tiles.

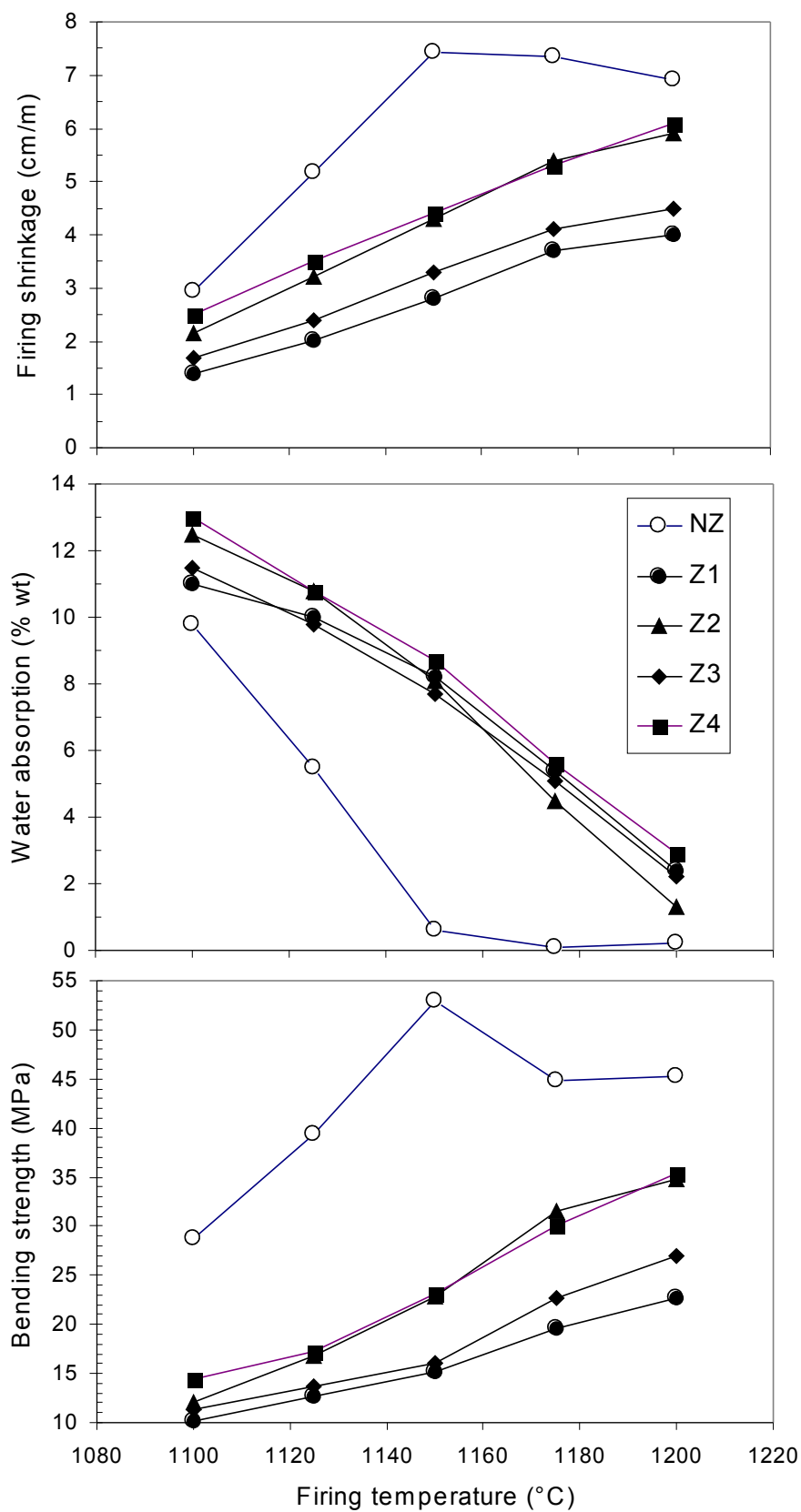


Fig. 4 Phase composition of zeolite-bearing tiles (Z5, Z6 and Z7) in comparison with a zeolite-free reference body (Z0).

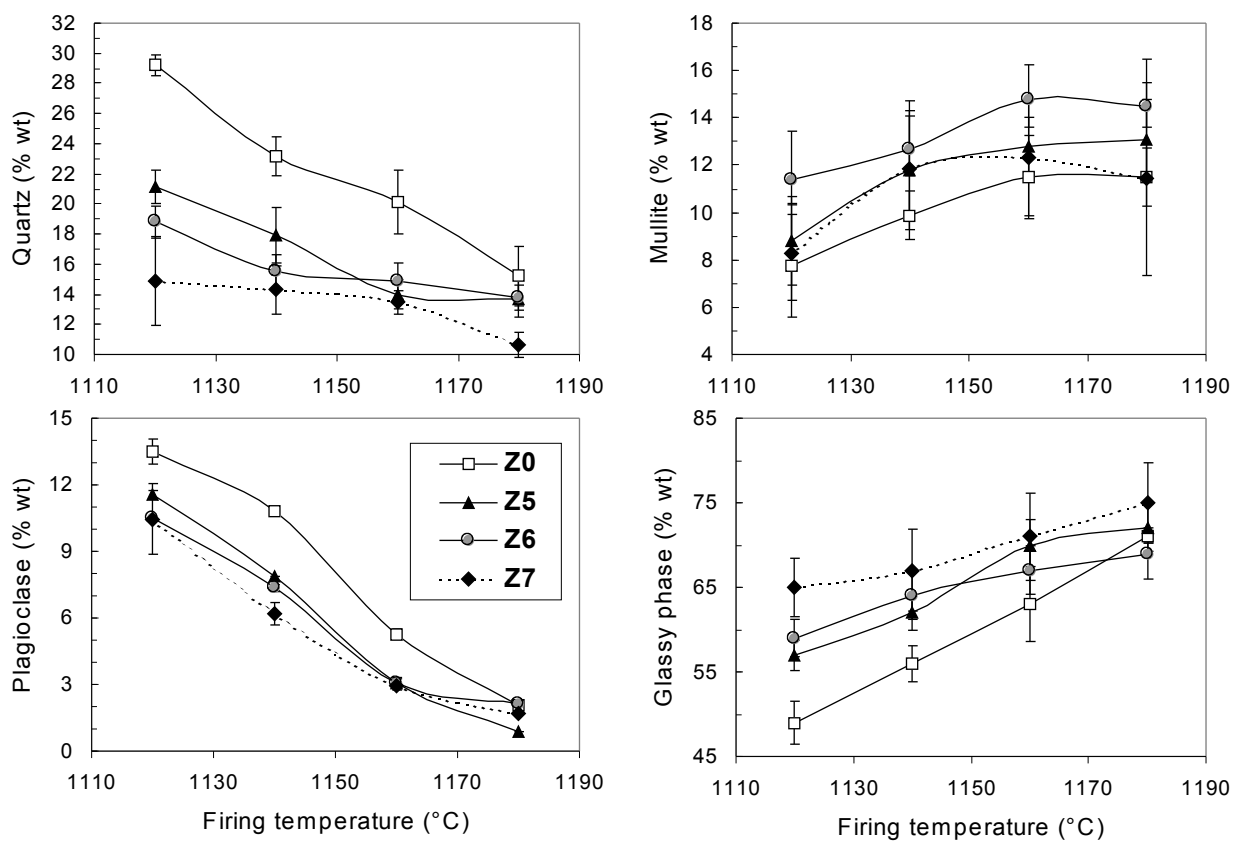


Fig. 5 Trends in chemical composition of the glassy phase formed during sintering of zeolite-bearing (Z5, Z6 and Z7) and zeolite-free (Z0) stoneware.

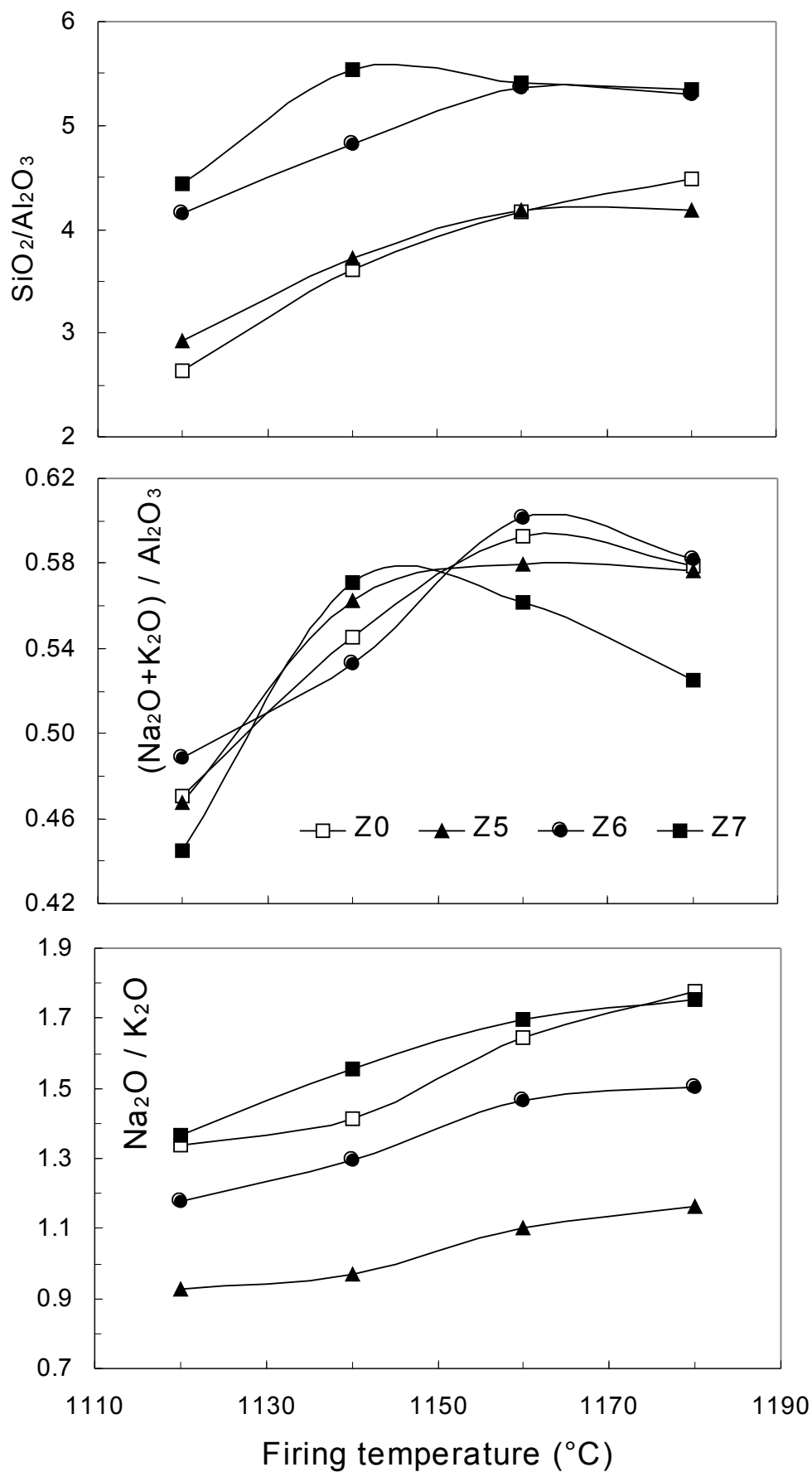


Table 1

Chemical composition of raw materials and ceramic bodies.

% wt.	Ball clays						Quartz-feldspathic fluxes				Ceramic bodies								
	F1	U1	U2	W1	W2	W3	AP	SF1	SF2	QFS	NZ	Z1	Z2	Z3	Z4	Z0	Z5	Z6	Z7
SiO ₂	64. 50	65. 80	57. 20	75.2 7	59. 40	61.0 6	71. 00	68. 20	69. 20	79. 20	70. 11	66.3 7	67. 26	66. 92	69. 53	66. 10	63. 14	65. 41	67. 48
TiO ₂	0.5 0	1.2 0	1.5 2	1.12 1.12	1.4 4	1.57 1.57	0.2 8	0.6 0	0.2 3	0.1 0	17. 21	17.3 3	17. 31	17. 47	16. 48	20. 49	20. 49	19. 67	18. 43
Al ₂ O ₃	22. 20	21. 00	27. 90	13.7 0	26. 70	25.2 4	16. 00	17. 60	18. 60	9.4 0	0.6 0	0.64 0.64	0.5 9	0.6 1	0.5 6	0.8 0	0.8 3	0.8 0	0.7 5
Fe ₂ O ₃	1.4 0	1.2 0	1.0 4	1.71 1.71	0.8 9	1.20 1.20	0.7 0	0.3 5	0.1 3	0.6 0	0.8 0	1.74 1.74	1.3 4	1.5 4	1.0 0	0.6 4	1.1 9	0.8 6	1.1 9
MgO	0.9 0	0.6 0	0.6 0	0.59 0.59	0.3 4	0.46 0.46	0.8 0	2.0 0	0.0 7	0.3 4	0.8 0	0.97 0.97	0.6 7	0.8 3	0.7 7	0.7 2	0.7 9	0.8 8	0.8 9
CaO	0.6 0	0.5 0	0.3 8	0.08 0.08	0.1 9	0.18 0.18	1.2 0	1.3 0	0.5 6	2.3 0	0.8 7	1.88 1.88	1.2 4	1.5 4	1.2 1	0.8 3	1.2 7	1.2 4	1.1 8
Na ₂ O	0.3 0	0.4 0	0.4 8	0.10 0.10	0.4 8	0.18 0.18	1.4 0	8.2 0	10. 40	2.0 0	4.1 7	3.40 3.40	3.6 9	3.6 5	3.4 8	4.2 2	3.5 3	3.3 2	3.4 9
K ₂ O	0.9 0	2.2 0	2.6 4	1.77 1.77	2.8 9	2.21 2.21	7.0 0	0.7 0	0.2 1	3.9 0	1.9 6	2.40 2.40	2.5 6	2.3 8	1.6 8	2.3 2	2.9 7	2.1 0	1.9 1
L.o.I.	8.5 0	6.8 0	7.6 8	5.68 5.68	7.3 0	7.90 7.90	1.5 0	1.0 0	0.5 4	2.1 0	3.3 9	5.28 5.28	5.2 7	4.7 8	5.0 0	3.7 1	5.6 3	5.3 6	4.5 6
Total	99. 80	99. 70	99. 44	100. 02	99. 63	100. 00	99. 88	99. 95	99. 94	99. 94	99. 91	100. 00	99. 92	99. 71	99. 71	99. 82	99. 84	99. 64	99. 88

Table 2
Formulation of ceramic bodies (% wt).

Bodies	Ball clays						Quartz-feldspathic materials				Zeolitites				
	F1	U1	U2	W1	W2	W3	AP	SF1	SF2	QFS	IS	TGN	IC	LB	ESC
NZ	10	15	-	15	-	-	10	20	20	10	-	-	-	-	-
Z1	10	15	-	15	-	-	-	10	20	10	20	-	-	-	-
Z2	10	15	-	15	-	-	-	10	20	10	-	20	-	-	-
Z3	10	15	-	15	-	-	-	10	20	10	-	-	20	-	-
Z4	10	15	-	15	-	-	-	10	20	10	-	-	-	20	-
Z0	-	-	15	-	15	10	10	20	20	10	-	-	-	-	-
Z5	-	-	15	-	15	10	-	20	10	10	-	20	-	-	-
Z6	-	-	15	-	15	10	-	20	10	10	-	-	-	20	-
Z7	-	-	15	-	15	10	-	20	10	10	-	-	-	-	20

Table 3
Chemico-physical characteristics of zeolitic rocks.

	IS	TGN	IC	LB	ESC
SiO ₂ (% wt.)	50.89 ± 0.73	55.34 ± 0.79	53.65 ± 0.77	66.68 ± 0.95	70.56 ± 1.01
TiO ₂	0.61 ± 0.05	0.40 ± 0.03	0.48 ± 0.04	0.25 ± 0.02	0.23 ± 0.02
Al ₂ O ₃	17.43 ± 0.57	17.30 ± 0.57	18.11 ± 0.60	13.17 ± 0.43	12.16 ± 0.40
Fe ₂ O ₃	5.21 ± 0.17	3.19 ± 0.10	4.19 ± 0.14	1.53 ± 0.05	3.08 ± 0.10
MgO	2.29 ± 0.07	0.79 ± 0.02	1.56 ± 0.05	1.27 ± 0.04	1.32 ± 0.04
CaO	6.30 ± 0.25	3.08 ± 0.12	4.60 ± 0.18	2.94 ± 0.11	2.57 ± 0.10
MnO	0.12 ± 0.01	0.13 ± 0.01	0.15 ± 0.02	0.02 ± 0.01	0.06 ± 0.01
SrO	0.17 ± 0.02	0.13 ± 0.01	0.08 ± 0.01	0.06 ± 0.01	0.05 ± 0.01
BaO	0.14 ± 0.02	0.05 ± 0.01	0.10 ± 0.01	0.11 ± 0.01	0.06 ± 0.01
Na ₂ O	0.96 ± 0.03	2.44 ± 0.08	2.24 ± 0.08	1.38 ± 0.05	2.31 ± 0.08
K ₂ O	6.04 ± 0.19	6.85 ± 0.22	5.96 ± 0.19	2.48 ± 0.08	1.86 ± 0.06
P ₂ O ₅	0.24 ± 0.04	0.12 ± 0.02	0.15 ± 0.03	0.03 ± 0.01	0.27 ± 0.05
L.o.I.	10.70 ± 0.10	10.63 ± 0.10	8.19 ± 0.10	9.29 ± 0.10	5.93 ± 0.10
Chabazite (% wt.)	61 ± 1	6 ± 1	48 ± 1		
Phillipsite		42 ± 1	12 ± 1		
Analcime		7 ± 1			
Clinoptilolite				66 ± 1	37 ± 1
Smectite	3 ± 1		7 ± 1		12 ± 1
Opal-CT				13 ± 1	8 ± 1
Volcanic glass	7 ± 1	21 ± 1	17 ± 1		
Feldspars	25 ± 1	24 ± 1	15 ± 1	18 ± 1	43 ± 1
Pyroxenes	3 ± 1				
Quartz				3 ± 1	traces
Biotite	1 ± 1	traces	1 ± 1	traces	traces
Specific surface (m ² ·g ⁻¹)	225 ± 10	120 ± 5	132 ± 6	52 ± 2	38 ± 1
C. E. C. (meq / 100g)	80.7 ± 3.5	129.9 ± 6.4	86.4 ± 5.6	64.2 ± 4.6	n.d.
exchangeable Na ⁺	7.2 ± 0.6	55.2 ± 0.9	18.4 ± 1.6	20.1 ± 1.7	n.d.
exchangeable K ⁺	29.6 ± 0.6	52.9 ± 4.1	45.6 ± 2.7	15.4 ± 0.3	n.d.
exchangeable Mg ²⁺	1.5 ± 0.1	0.4 ± 0.1	0.8 ± 0.1	4.6 ± 0.4	n.d.
exchangeable Ca ²⁺	42.0 ± 2.2	21.0 ± 1.3	21.4 ± 1.1	23.5 ± 2.2	n.d.
exchangeable Sr ²⁺	0.4 ± 0.1	0.3 ± 0.1	0.1 ± 0.1	0.3 ± 0.1	n.d.
exchangeable Ba ²⁺	0.1 ± 0.1	<0.1	<0.1	0.3 ± 0.1	n.d.

n.d. = not determined.

Table 4

Fusibility of zeolitic rocks in comparison with conventional feldspathic fluxes [Dondi et al. 2001].

Material	Characteristic temperatures (°C)			BI Bloating index
	T_2 End of sintering	T_3 Initial softening	T_4 Half sphere	
Zeolitite IS	1200 ± 10	1220 ± 10	1320 ± 10	1.5 ± 0.1
Zeolitite IC	1200 ± 10	1230 ± 10	1365 ± 10	1.1 ± 0.1
Zeolitite TGN	1150 ± 10	1200 ± 10	1385 ± 10	1.8 ± 0.1
Zeolitite LB	1200 ± 10	1250 ± 10	1460 ± 10	2.0 ± 0.1
Zeolitite ESC	1230 ± 10	1280 ± 10	1470 ± 10	1.6 ± 0.1
Nepheline syenite	1240-1270	1270-1310	1370-1400	1.1-1.2
Sodic feldspar	1260-1300	1300-1330	1430-1490	1.0-1.4
Potassic feldspar	1300-1350	1370-1390	1570-1600	1.2-1.9

Table 5
Technological behaviour of unfired tiles.

Technological parameter	Unit	NZ	Z1	Z2	Z3	Z4	Z0	Z5	Z6	Z7
Working moisture	% wt.	7.2 ± 0.1	6.4 ± 0.1	6.4 ± 0.1	6.5 ± 0.1	6.0 ± 0.1	5.9 ± 0.1	5.2 ± 0.1	6.4 ± 0.1	5.1 ± 0.1
Compressibility of powders	adim.	n.d.	n.d.	n.d.	n.d.	n.d.	3.0 ± 0.2	2.7 ± 0.1	2.7 ± 0.1	2.9 ± 0.1
Pressing expansion	cm·m ⁻¹	0.4 ± 0.1	0.3 ± 0.1	0.4 ± 0.1	0.3 ± 0.1	0.5 ± 0.1	0.7 ± 0.1	0.7 ± 0.1	0.7 ± 0.1	0.8 ± 0.1
Green modulus of rupture	MPa	0.7 ± 0.1	1.1 ± 0.2	0.8 ± 0.1	0.9 ± 0.1	1.0 ± 0.2	0.9 ± 0.1	0.9 ± 0.1	1.0 ± 0.1	0.9 ± 0.1
Dry modulus of rupture	MPa	2.6 ± 0.3	2.1 ± 0.1	2.0 ± 0.3	1.8 ± 0.2	2.1 ± 0.1	2.2 ± 0.2	2.4 ± 0.1	2.7 ± 0.2	1.5 ± 0.1
Drying shrinkage	cm·m ⁻¹	-0.3 ± 0.1	-0.3 ± 0.1	-0.4 ± 0.1	-0.3 ± 0.1	-0.5 ± 0.1	-0.3 ± 0.1	-0.2 ± 0.1	-0.2 ± 0.1	-0.1 ± 0.1

n.d. = not determined.

Table 6

Technological behaviour of fired tiles.

Body	Firing temperature °C	Firing shrinkage cm·m ⁻¹	Water absorption % weight	Bulk density g·cm ⁻³	Open porosity % volume	Closed porosity % volume	Modulus of rupture MPa
Z0 (reference)	1120	4.6 ± 0.1	5.9 ± 0.2	2.18 ± 0.01	12.9 ± 0.4	3.4 ± 0.5	41.9 ± 1.1
	1140	6.7 ± 0.1	1.6 ± 0.1	2.33 ± 0.01	3.8 ± 0.2	2.0 ± 0.5	49.6 ± 3.4
	1160	7.4 ± 0.1	0.16 ± 0.03	2.39 ± 0.01	0.4 ± 0.1	3.3 ± 0.5	50.2 ± 3.2
	1180	7.0 ± 0.1	0.15 ± 0.04	2.37 ± 0.01	0.4 ± 0.1	4.4 ± 0.5	42.2 ± 3.6
Z5 (TGN)	1120	6.3 ± 0.1	5.5 ± 0.3	2.15 ± 0.01	11.8 ± 0.6	3.3 ± 0.5	30.7 ± 1.3
	1140	8.0 ± 0.1	1.5 ± 0.1	2.27 ± 0.01	3.3 ± 0.3	3.0 ± 0.5	32.1 ± 1.1
	1160	8.3 ± 0.1	0.2 ± 0.1	2.30 ± 0.01	0.5 ± 0.1	5.1 ± 0.5	29.2 ± 2.5
	1180	7.8 ± 0.1	0.12 ± 0.06	2.25 ± 0.01	0.3 ± 0.1	7.0 ± 0.5	27.6 ± 2.1
Z6 (LB)	1120	6.8 ± 0.1	6.3 ± 0.3	2.11 ± 0.01	13.4 ± 0.6	0.5 ± 0.5	27.9 ± 2.0
	1140	8.3 ± 0.1	2.5 ± 0.2	2.23 ± 0.01	5.7 ± 0.5	1.9 ± 0.5	32.3 ± 1.0
	1160	9.1 ± 0.1	0.6 ± 0.1	2.29 ± 0.01	1.4 ± 0.3	3.7 ± 0.5	30.5 ± 2.1
	1180	9.2 ± 0.1	0.2 ± 0.1	2.30 ± 0.01	0.6 ± 0.2	4.7 ± 0.5	29.7 ± 1.7
Z7 (ESC)	1120	7.1 ± 0.1	3.7 ± 0.3	2.25 ± 0.01	8.4 ± 0.7	2.9 ± 0.5	45.0 ± 0.9
	1140	8.6 ± 0.1	0.6 ± 0.1	2.36 ± 0.01	1.5 ± 0.2	3.9 ± 0.5	51.8 ± 2.1
	1160	8.8 ± 0.1	0.08 ± 0.06	2.41 ± 0.01	0.2 ± 0.1	3.1 ± 0.5	47.2 ± 3.0
	1180	8.7 ± 0.1	0.08 ± 0.03	2.38 ± 0.01	0.2 ± 0.1	3.6 ± 0.5	41.0 ± 2.0

Table 7

Comparison of the zeolite content of ceramic bodies and the main technological features of porcelain stoneware tiles at maximum densification.

Body	Zeolite content % weight	Loss on Ignition % weight	Firing temperature °C	Firing shrinkage cm·m ⁻¹	Bulk density g·cm ⁻³	Open porosity % volume	Closed porosity % volume	Modulus of rupture MPa
Z0 (reference)	0.0	3.71	1160	7.4	2.39	0.4	3.3	50.2
Z5 (TGN)	11.0	5.63	1160	8.3	2.30	0.5	5.1	29.2
Z6 (LB)	13.2	5.36	1180	9.2	2.30	0.6	4.7	29.7
Z7 (ESC)	7.4	456	1160	8.8	2.41	0.2	3.1	47.2

Table 8

Chemical composition and calculated physical properties of the glassy phase in porcelain stoneware tiles in function of firing temperature (°C).

% wt.	Z0				Z5				Z6				Z7			
	1120	1140	1160	1180	1120	1140	1160	1180	1120	1140	1160	1180	1120	1140	1160	1180
SiO ₂	60.8	66.6	69.0	70.8	62.3	66.1	68.3	68.3	69.3	71.6	72.6	72.7	71.3	73.4	73.2	73.6
TiO ₂	1.6	1.4	1.2	1.1	1.5	1.4	1.3	1.2	1.4	1.3	1.3	1.2	1.2	1.2	1.1	1.0
Al ₂ O ₃	23.0	18.5	16.6	15.8	21.3	17.7	16.3	16.4	16.7	14.9	13.6	13.7	16.1	13.2	13.5	13.8
Fe ₂ O ₃	1.4	1.2	1.1	1.0	2.2	2.0	1.8	1.7	1.5	1.4	1.4	1.3	1.9	1.8	1.8	1.6
MgO	1.5	1.3	1.2	1.0	1.5	1.3	1.2	1.2	1.6	1.5	1.4	1.3	1.4	1.4	1.3	1.2
CaO	0.9	0.9	1.1	1.1	1.3	1.5	1.7	1.8	1.2	1.4	1.7	1.7	1.1	1.4	1.5	1.5
Na ₂ O	6.2	5.9	6.1	5.9	4.8	4.9	5.0	5.1	4.4	4.5	4.8	4.8	4.1	4.6	4.8	4.6
K ₂ O	4.6	4.2	3.7	3.3	5.2	5.1	4.5	4.4	3.8	3.4	3.3	3.2	3.0	3.0	2.8	2.6
Viscosity (MPa·s)	11.93	7.00	4.35	3.33	15.59	8.42	5.57	4.02	14.68	9.23	5.73	4.36	14.98	8.24	5.83	4.55
Surface tension (N·m ⁻¹)	0.357	0.349	0.347	0.348	0.355	0.348	0.348	0.350	0.348	0.346	0.345	0.348	0.348	0.343	0.346	0.349